Tunable amplification and absorption properties in double-Λ system of GaAs/AlGaAs multiple quantum wells

YAN Wei, WANG Tao[*], LI XiaoMing & JIN YaJuan

Wuhan National Laboratory for Optoelectronics, College of Optoelectronic Science and Engineering, Huazhong University of Science and Technology, Wuhan 430074, China

We study the optical amplification and absorption properties in a double-Λ four level system of GaAs/AlGaAs multiple quantum wells (MQWs) under realistic experimental conditions. The amplification and absorption responses of two weak fields can be achieved by adjusting the relative phase, the probe detuning, and the two pump Rabi frequencies appropriately. The investigation is much more practical than its atomic counterpart because of its flexible design and the wide adjustable parameters. It may provide a new possibility in technological applications for the light amplifier working on quantum coherence effects in MQWs solid-state system.

multiple quantum wells, optical amplification and absorption, GaAs/AlGaAs

In recent years, semiconductor quantum wells has drawn significant attention for the reasons that it can be viewed as the two dimensional electron gas, having properties similar to atomic vapors such as the discrete levels. Due to the small effective electron mass, it has advantages of high nonlinear optical coefficients and large electric dipole moments. Several typical interesting phenomena such as electromagnetically induced transparency (EIT) [1–5], lasing without inversion [6], highly efficient four-wave mixing [7], all-optical switching [8], and slow light [1] have been demonstrated. As a method to study quantum coherent control and interference, the relative phase of the applied laser fields has been widely used, which is usually termed as phase control, in several important processes in atomic, molecular, and solid-state systems [9–14], but the study of amplification and absorption properties in double-Λ system of GaAs/AlGaAs MQWs has not been reported.

In this paper, we study controllable optical amplification and absorption responses of the probe and the signal laser fields in a double-Λ four-level system on GaAs/AlGaAs

MQWs under realistic experimental conditions [1,3,15]. The main advantages of applying our considered MQWs scheme over other approaches are as follows. The MQWs medium studied here is a solid, which is much more practical than that in gaseous medium due to its flexible design and the wide adjustable parameters. The MQWs medium here provides a highly tunable quantum system. The quantum properties of these nanostructures such as the transition energies and dipole moments can be well-manipulated by accurately tailoring their shapes and sizes while they can hardly be found in the models for cold atom media.

1   Theoretical framework

Our studies to realize the double-Λ four-level system in semiconductor MQWs have exploited the use of exciton spin coherence. For semiconductors such as a GaAs MQWs, the interband optical transitions are characterized by excitonic transitions between the doubly degenerate conduction bands with $s=\pm1/2$ and the doubly degenerate heavy-hole (HH) and light-hole (LH) valence bands with $j_z=\pm3/2$ and

*Corresponding author (email: wangtao@hust.edu.cn)

$j_z=\pm 1/2$, respectively. For the HH excitonic transitions, spin-up $|+>$ (σ^+ transition) and spin-down $|->$ (σ^- transition) exciton can be excited with σ^+ and σ^- circularly polarized light, respectively, as shown in Figure 1(a). Although the $|+>$ and $|->$ exciton share no common states, these excitons can interact with each other via Coulomb correlations, leading to the formation of bound and unbound (but still correlated) two-exciton states. Exciton spin coherence (coherent superposition of the $|+>$ and $|->$ states) can be induced via the exciton to two-exciton transition with opposite spins. The exciton states $|+>$ and $|->$, the unbound two-exciton state $|+->_u$, and bound two-exciton state $|+->_b$ resemble a double-Λ four level system, as shown in Figure 1(b). The bound and unbound two-exciton transitions are separated by 2 meV [8,15]. Since both of the exciton states are initially unoccupied, we prepared on initial population in the $|+>$ state by applying a σ^+ polarized prepulse to the $|+>$ excitonic [1,4,8].

For simplification, we denote the two exciton states ($|+>$ and $|->$) by $|1>$ and $|2>$, respectively, and treat the two-exciton states ($|+->_b$ and $|+->_u$) as a single level by $|3>$ and $|4>$, and allow each laser pulse to drive only on transition. The MQWs system interacts with two strong laser fields (called pump-c and pump-d) and two weak laser fields (called the probe and signal) coupling respectively $|2>\leftrightarrow|3>$, $|2>\leftrightarrow|4>$, $|1>\leftrightarrow|3>$, and $|1>\leftrightarrow|4>$. The GaAs/Al$_{0.35}$Ga$_{0.65}$As MQWs structure, considered here, consists of twenty periods of wells (GaAs) and barriers (AlGaAs) with a thickness of 9 and 20 nm, respectively.

Under the rotating-wave approximation and dipole approximation, in the Schrödinger picture the free and the interaction Hamiltonian for such a double-Λ system can be written respectively as (with the assumption $\hbar=1$) [16,17]

$$H_0 = \omega_p|3><3| + (\omega_p - \omega_c)|2><2| + (\omega_p - \omega_c + \omega_d)|4><4|, \tag{1}$$

$$H_{int}^S = -\Omega_p e^{-i(\omega_p t - \phi_p)}|3><1| - \Omega_c e^{-i(\omega_c t - \phi_c)}|3><2| - \Omega_d e^{-i(\omega_d t - \phi_d)}|4><2| - \Omega_s e^{-i(\omega_s t - \phi_s)}|4><1| + H.c., \tag{2}$$
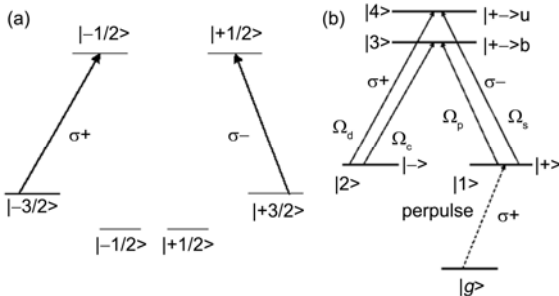

Figure 1 (a) Schematic energy-level diagram for a GaAs quantum well, along with the circular polarization selection rules for the HH exciton transition. (b) Double Λ system in biexciton transition with ground state $|g>$, single exciton states $|+>$ and $|->$, bound biexciton state $|+->_b$, and unbound biexciton state $|+->_u$.

where ϕ_j (j=p, c, d and s) is the absolute phase of the field j. *H.c.* is the Hermitian conjugate. Turning to the interaction picture, when the carrier frequencies fulfill the relation $\omega_p+\omega_d=\omega_s+\omega_c$, the resulting interaction Hamiltonian can be written as

$$H_{int}^I = \Delta_p|3><3| + (\Delta_p - \Delta_c)|2><2| + (\Delta_p - \Delta_c + \Delta_d)|4><4| - (\Omega_p e^{i\phi_p}|3><1| + \Omega_c e^{i\phi_c}|3><2| + \Omega_d e^{i\phi_d}|4><2| + \Omega_s e^{i\phi_s}|4><1| + H.c.), \tag{3}$$

where $\Delta_p=\omega_{31}-\omega_p$, $\Delta_c=\omega_{32}-\omega_c$, and $\Delta_d=\omega_{42}-\omega_d$ are the single-photon detunigs (ω_{31}, ω_{32}, and ω_{42} are the frequency of the $|3>\leftrightarrow|1>$, $|3>\leftrightarrow|2>$, and $|4>\leftrightarrow|2>$, respectively). The relation $\omega_p+\omega_d=\omega_s+\omega_c$ is reduced to $\Delta_p+\Delta_d=\Delta_s+\Delta_c$ with $\Delta_s=\omega_{41}-\omega_s$ also being the single-photon detuning. Ω_m (m=p, c, d, s) denotes the Rabi frequency of the laser field for the relevant laser-driven transitions. We define the exciton energy state as

$$|\psi> = A_1|1> + A_2 e^{i(\phi_p-\phi_c)}|2> + A_3 e^{i\phi_p}|3> + A_4 e^{i\phi_s}|4>. \tag{4}$$

The A_j (j=1–4) stands for the time-dependent probability amplitude of finding the exciton and biexciton in the level $|j>$. Making use of Schrödinger equation

$$i\frac{\partial \psi}{\partial t} = H_{int}^I \psi \tag{5}$$

and eq. (4), the equations of motion for the probability amplitude of the exciton and biexciton wave functions can be readily obtained as

$$\frac{\partial A_1}{\partial t} = iA_3\Omega_p + iA_4\Omega_s, \tag{6a}$$

$$\frac{\partial A_2}{\partial t} = iA_2[(\Delta_c - \Delta_p) + ir_2] + iA_3\Omega_c + iA_4\Omega_d e^{-i\phi}, \tag{6b}$$

$$\frac{\partial A_3}{\partial t} = iA_1\Omega_p + iA_2\Omega_c + i(-\Delta_p + ir_3)A_3, \tag{6c}$$

$$\frac{\partial A_4}{\partial t} = iA_1\Omega_s + iA_4[(\Delta_c - \Delta_p - \Delta_d) + ir_4] + iA_2\Omega_d e^{i\phi}, \tag{6d}$$

where r_3 and r_4 are the decoherence rate for both dipole transitions, and r_2 is the nonradiative decoherence rate [1–5]. We define $\phi=\phi_p+\phi_d-\phi_c-\phi_s$ which is the relative phase of laser field p, c, d and s.

In the limit of weak probe and signal fields, almost all excitons will remain in the level $|1>$. Hence, we assume that $|A_1|^2 \approx 1$. Under this assumption, we can obtain straightforwardly the steady-state solutions of eq. (6). And the slowly varying parts of the polarizations of the probe and the signal ($P_p=\varepsilon_0\chi_p E_p=N\mu_{13}A_3A_1^*$ and $P_s=\varepsilon_0\chi_s E_s=N\mu_{14}A_4A_1^*$), the susceptibilities of the probe and signal can be written as

$$\chi_p = \frac{N|\mu_{13}|^2}{\hbar\varepsilon_0\Omega_p}A_3A_1^* = \frac{N|\mu_{13}|^2}{\hbar\varepsilon_0}\chi_p', \tag{7a}$$

$$\chi_s = \frac{N|\mu_{14}|^2}{\hbar\varepsilon_0\Omega_s}A_4A_1^* = \frac{N|\mu_{14}|^2}{\hbar\varepsilon_0}\chi_s', \tag{7b}$$

where N is the density of carriers and μ_{13} (μ_{14}) is the dipole matrix element between |1> and |3> (|4>). Then we can readily obtain

$$\chi'_p = \frac{A_3}{\Omega_p} = \frac{\Omega_d^2 - b_1 b_3 - \Omega_c \Omega_d \Omega_s e^{-i\phi} / \Omega_p}{b_1 b_2 b_3 - b_3 \Omega_c^2 - b_2 \Omega_d^2}, \qquad (8a)$$

$$\chi'_s = \frac{A_4}{\Omega_s} = \frac{\Omega_c^2 - b_1 b_2 - \Omega_c \Omega_d \Omega_p e^{i\phi} / \Omega_s}{b_1 b_2 b_3 - b_3 \Omega_c^2 - b_2 \Omega_d^2}. \qquad (8b)$$

Here $b_1 = \Delta_c - \Delta_p + ir_2$, $b_2 = -\Delta_p + ir_3$, and $b_3 = \Delta_c - \Delta_p - \Delta_d + ir_4$.

2 Tunable amplification and absorption

In this section, we will study the dependence of the susceptibilities of the probe and the signal fields on the pump Rabi frequencies, and the relative phase ϕ based on eq. (8) and show how these parameters are used to control the amplification and absorption of the two weak fields. As we all know, the $\text{Im}(\chi_p)$ and $\text{Im}(\chi_s)$ correspond to absorption or amplification. If $\text{Im}(\chi_p) < 0$ ($\text{Im}(\chi_s) < 0$), the probe (signal) field will be amplified. On the contrary, if $\text{Im}(\chi_p) > 0$ ($\text{Im}(\chi_s) > 0$), the probe (signal) field will be absorbed [9,18,19].

In Figure 2, we plot the absorption and amplification response of the probe field (see Figure 2(a)) and the signal field (see Figure 2(b)), versus the probe detuning Δ_p with different pump-c and pump-d Rabi frequencies. The solid, dashed, and dotted curves correspond to $\Omega_c = \Omega_d = 3$ THz, $\Omega_d = 2\Omega_c = 3$ THz, and $\Omega_c = 2\Omega_d = 3$ THz, respectively. As shown in the figure, the susceptibilities of the two fields depend so sensitively on the ratio of the pump Rabi frequencies that the corresponding profiles are quite different. When $\Omega_c = 2\Omega_d = 3$ THz, the amplification of the probe field can be achieved, while for the signal, there are three absorption peaks. Contrarily, for the case $\Omega_d = 2\Omega_c = 3$ THz, the absorption spectrum of the probe field exhibits three peaks, whereas the amplification of the signal can be achieved. When $\Omega_c = \Omega_d = 3$ THz, both fields exhibit transparency except for two steep absorption peaks at about $\Delta_p = \pm 4.3 \times 10^{11}$ Hz.

In order to further show explicitly the dependence of the amplification-absorption responses of the probe and the signal on the pump Rabi frequencies, we give the density plot in Figure 3, that correspond to Figure 2(a). In Figure 3, we choose the pump-c Rabi frequencies as 3 THz in Figure 3(a), and 1.5 THz in Figure 3(b) to address how the linear susceptibility of the probe is influenced by the probe detuning Δ_p and the pump-d Rabi frequency. As shown in the figure, the amplification only can be obtained at a certain
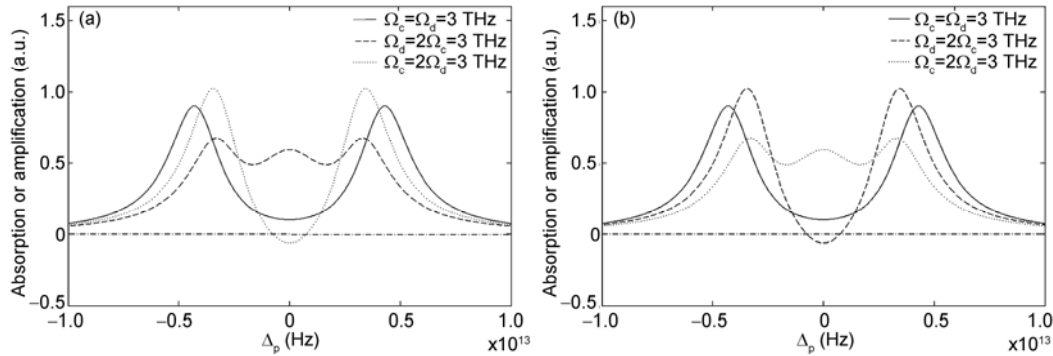

Figure 2   The amplification-absorption responses. (a) $\text{Im}(\chi'_p)$ and (b) $\text{Im}(\chi'_s)$ versus the probe detuning Δ_p with different ratios of the pump-c Rabi frequency Ω_c to the pump-d Rabi frequency Ω_d. Other parameters are $\Delta_c = \Delta_d = 0$, $\phi = 0$, $r_2 = 0.8 \times 10^{12}$ Hz, $r_3 = r_4 = 2 \times 10^{12}$ Hz, and $\Omega_s = \Omega_p$, respectively.
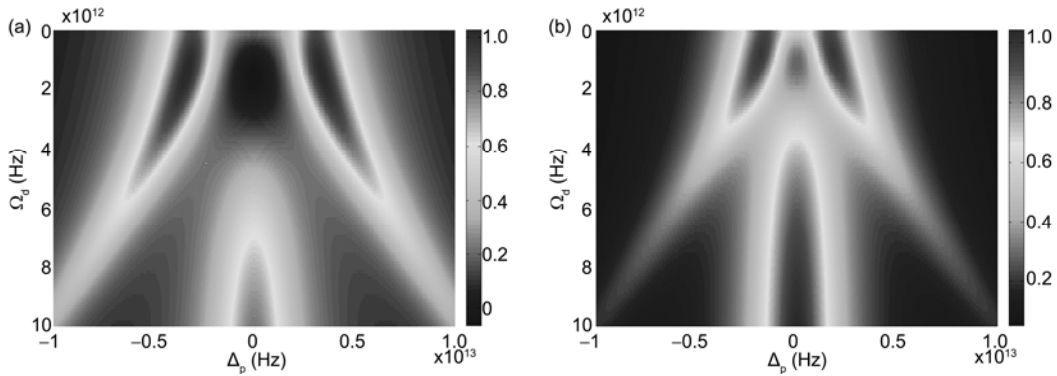

Figure 3   Density of the amplification-absorption response $\text{Im}(\chi'_p)$ versus the probe detuning Δ_p and the pump-d Rabi frequency Ω_d for the fixed pump-c Rabi frequency. (a) $\Omega_c = 3$ THz; (b) $\Omega_c = 1.5$ THz. Other parameters are the same as in Figure 2.

range of detuning [-0.7×10^{12} Hz, 0.7×10^{12} Hz] and of pump-d [0.8×10^{12} Hz, 2.2×10^{12} Hz] (see the Figure 3(a)), and the three peaks of absorption is more obvious at $\Omega_c=3$ THz than $\Omega_c=1.5$ THz. The signal field is similar with probe field, and here we do not discuss it. Therefore, the amplification and absorption of the two weak fields can be achieved by adjusting the pump-d and the probe detuning.

In Figure 4, we display the amplification-absorption response (a) Im(χ'_p) and (b) Im(χ'_s) as a function of the probe detuning Δ_p with different values of the relative phase ϕ. The solid, dashed, and dotted curves correspond respectively to $\phi=0$, $\phi=\pi/2$, and $\phi=3\pi/2$. Other parameters are $\Delta_c=\Delta_d=0$, $r_2=0.8\times10^{12}$ Hz, $r_3=r_4=2\times10^{12}$ Hz, $\Omega_c=\Omega_d=3$ THz, and $\Omega_s=\Omega_p$, respectively. It can be found that, the amplification of the probe and signal fields can be achieved for a wide region of probe detuning and they are quite sensitive to the relative phase ϕ. As shown in this figure, when $\phi=0$, neither the probe nor the signal exhibits amplification. While $\phi=\pi/2$, the absorption spectrum of the probe shows amplification for a wide region of negative probe detuning, and yet the absorption spectrum of the signal shows amplification for a wide region of positive probe detuning. Contrarily, when the relative phase $\phi=3\pi/2$, the absorption spectrum of the probe shows amplification for a wide region of

positive probe detuning, while the absorption spectrum of the signal exhibits amplification for a wide region of negative probe detuning. Furthermore, both the absorption spectra of the probe and signal fields exhibit symmetry with respect of $\Delta_p=0$. According to what has been discussed above, we can arrive at the conclusion that the amplification-absorption spectra are so sensitive to the relative phase ϕ that we can obtain the light field amplification by adjusting the value of the relative phase appropriately. For example, when $\Delta_p=-0.5--0.1$ THz, we can switch the probe response from an intense absorption to a great amplification just by changing the relative phase ϕ from 0 to $\pi/2$. At the same time, we can switch the signal response from the high absorption to large amplification just by modulating the relative phase ϕ from 0 to $3\pi/2$.

To get a deeper insight into the influence of the single-photon probe detuning Δ_p and relative phase ϕ on the amplification-absorption response, we present the density plots in Figure 5. As we have done in Figure 4, we take $\Omega_c=\Omega_d=3$ THz, and $\Omega_s=\Omega_p$. As can be seen from the figure, the Im(χ'_p) and Im(χ'_s) are periodically phase-dependent and the periods are both 2π. When $\phi=0$ or $2k\pi$ ($k=\pm1$, $\pm2,\ldots$), the absorption spectra of the probe and signal fields exhibit double-peak structure. When $\phi=\pi/2$ or $k\pi+\pi/2$, the
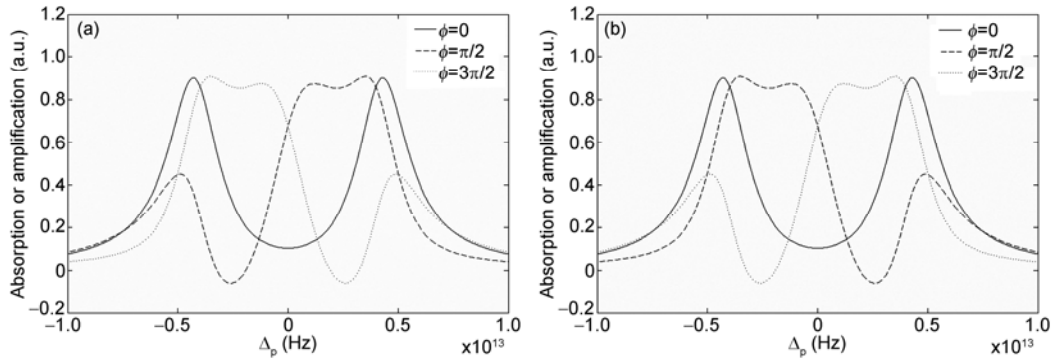

Figure 4　The amplification-absorption responses. (a) Im(χ'_p) and (b) Im(χ'_s) as a function of the probe detuning Δ_p with different values of the relative phase ϕ. Other parameters are $\Delta_c=\Delta_d=0$, $r_2=0.8\times10^{12}$ Hz, $r_3=r_4=2\times10^{12}$ Hz, $\Omega_c=\Omega_d=3$ THz and $\Omega_s=\Omega_p$, respectively.
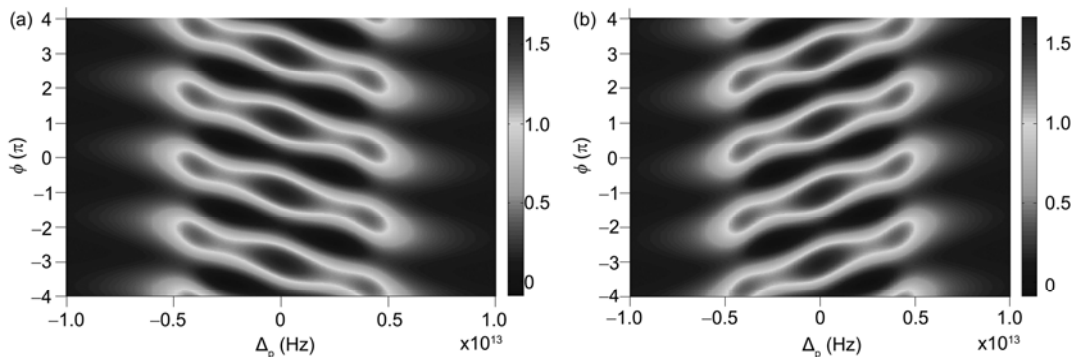

Figure 5　Density plots of the amplification-absorption responses (a) Im(χ'_p) and (b) Im(χ'_s) as a function of the probe detuning Δ_p and the relative phase ϕ. Other parameters are $\Delta_c=\Delta_d=0$, $r_2=0.8\times10^{12}$ Hz, $r_3=r_4=2\times10^{12}$ Hz, $\Omega_c=\Omega_d=3$ THz and $\Omega_s=\Omega_p$, respectively.

amplification appear for probe and signal fields. From Figures 4 and 5, we can get that the amplification and absorption of the two weak fields can be achieved by adjusting the relative phase ϕ and probe detuning Δ_p.

In Figure 6, we plot the amplification-absorption responses of the probe and signal, $\text{Im}(\chi'_p)$ (see Figure 6(a)) and $\text{Im}(\chi'_s)$ (see Figure 6(b)), versus the relative phase ϕ with different pump-c and pump-d Rabi frequencies. The solid, dashed, and dotted curves correspond respectively to $\Omega_c=\Omega_d=3$ THz, $\Omega_d=2\Omega_c=3$ THz, and $\Omega_c=2\Omega_d=3$ THz. From the two figures, it can obviously be seen that $\text{Im}(\chi'_p)$ and $\text{Im}(\chi'_s)$ are periodically phase-dependent and their periods are 2π. And the amplification of the probe and signal both occur in the range of $[2k\pi-0.2\pi, 2k\pi+0.2\pi]$. Furthermore, for the probe field, only $\Omega_c=2\Omega_d=3$ THz can be amplified (see the dotted line in Figure 6(a)). When $\Omega_d=2\Omega_c=3$ THz, the probe absorption is larger than that of the rest two cases. While for the signal field, the situation is just on the contrary, only when $\Omega_d=2\Omega_c=3$ THz can it be amplified. And when $\Omega_c=2\Omega_d=3$ THz, the signal absorption is larger than that of the other two cases. This is to say, we can obtain the amplification of the probe and signal by exchanging the values of the pump-c and pump-d Rabi frequencies. For the case $\Omega_c=\Omega_d=3$ THz, both fields are absorbed. This can be verified from the analytical expressions of eq. (8).

In order to further show explicitly the dependence of the amplification-absorption responses of the probe field on the pump-c and pump-d Rabi frequencies. We give the density plots in Figure 7 that correspond to Figure 6(a). In Figure 7, we choose the pump-c Rabi frequency as 3 THz in Figure 7(a), and 1.5 THz in Figure 7(b) to address how the linear susceptibility of the probe is influenced by the relative phase ϕ and the pump-d Rabi frequency Ω_d. As we have obtained from Figure 6(a), $\text{Im}(\chi'_p)$ is periodically phase-dependent and the period is 2π. In addition, when $\Omega_c=3$ THz the probe amplification can be achieved near $2k\pi$, and the maximum of the amplification is obtained probably 1.8 THz (the deepest in Figure 7(a)). While in Figure 7(b) $\Omega_c=1.5$ THz, only the absorption appears. This is consistent with the description of the solid and dotted curves in Figure 6(a). The signal field is similar with probe, and here we do not dicusss it. Therefore, large absorption and amplification of the two weak fields can be realized by controlling the relative phase ϕ and the pump-d Rabi frequency.

3   Conclusion

By solving analytically the steady-state Schrödinger equations we have demonstrated relative phase, probe detuning,
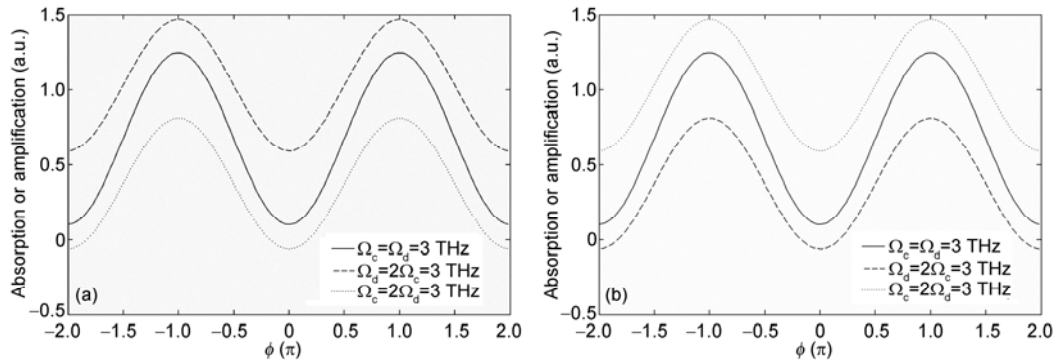

Figure 6   The amplification-absorption responses. (a) $\text{Im}(\chi'_p)$ and (b) $\text{Im}(\chi'_s)$ versus the relative phase ϕ with different ratios of the pump-c Rabi frequency Ω_c to the pump-d Rabi frequency Ω_d. Other parameters are $\Delta_p=\Delta_c=\Delta_d=0$, $r_2=0.8\times10^{12}$ Hz, $r_3=r_4=2\times10^{12}$ Hz, and $\Omega_s=\Omega_p$, respectively.

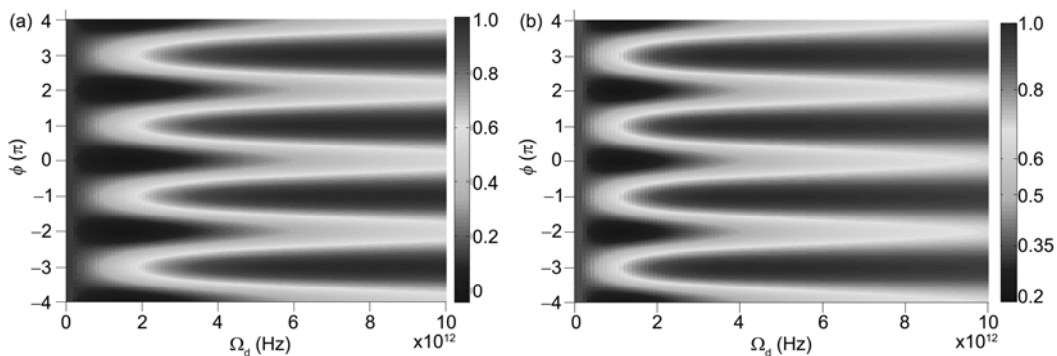**Figure 7**   Density plot of the amplificaiton-absorption response $\text{Im}(\chi'_p)$ versus the realvive phase ϕ and the pump-d Rabi frequency Ω_d for the fixed pump-c Rabi frequency Ω_c. (a) $\Omega_c=3$ THz; (b) $\Omega_c=1.5$ THz. Other parameters are the same as in Figure 6.

and pump (c,d) Rabi frequencies control of the linear susceptibilities for the probe and signal fields in a double-Λ system of GaAs/AlGaAs MQWs, which is a novel scheme to study manipulation amplification-absorption response in semiconductor regime. The results show that the amplification of the two weak fields, could be realized by properly changing the relative phase, the probe detuning, and the Rabi frequencies of the pump-c and pump-d. This study is much more practical than its atomic counterpart due to its flexible design and the wide adjustable parameters. Finally, we would like to point out that all the parameters are based on the experiment, and thus we believe it may provide a new possibility in technological applications for the light amplifier working on quantum coherence effects in MQWs solid-state system.

1 Ma S M, Xu H, Ham B S. Electromagnetically-induecd transparency and slow light in GaAs/AlGaAs multiple quantum well in a transient regime. Opt Express, 2009, 17: 14902–14908

2 Phillips M C, Wang H L. Spin coherence and electromagnetically induced transparency via exciton correlations. Phys Rev Lett, 2002, 89: 186401

3 Phillips M C, Wang H L. Electromagnetically induced transparency in semiconductors via biexciton coherence. Phys Rev Lett, 2003, 91: 183602

4 Phillips M C, Wang H L. Exciton spin coherence and electromagnetically induced transparency in the transient optical response of GaAs quantum wells. Phys Rev B, 2004, 69: 115337

5 Phillips M C, Wang H L. Electromagnetically induced transparency due to intervalence band coherence in a GaAs quantum well. Opt Lett, 2002, 28: 831–833

6 Frogley M D, Dynes J F, Beck M, et al. Gain without inversion in semiconductor nanostructures. Nat Mater, 2006, 5: 175–178

7 Wu Y, Saldana J, Zhu Y. Large enhancement of four-wave mixing by suppression of photon absorption from electromagnetically induced transparency. Phys Rev A, 2003, 67: 013811

8 Kang H, Park Y H, Sohn I B. All-optical switching with a biexcitonic double lambda system. Opt Commun, 2011, 284: 1045–1052

9 Wang L G, Qamar S, Zhu S Y, et al. Manipulation of the Raman process via incoherent pump, tunable intensity, and phase control. Phys Rev A, 2008, 77: 033833

10 Hao X Y, Ding C L, Lu X Y, et al. Controlled amplification, absorption, and dispersion of weak far-infrared lights in a coupled-quantum-well structure. Physica E, 2010, 42: 1984–1989

11 Sun H, Niu Y P, Jin S Q, et al. Phase control of cross-phase modulation with electromagnetically induce transparency. J Phys B, 2007, 40: 3037–3043

12 Peng Y G, Zheng Y J. Photon statistics of V-type three-level system in single quantum dots. Appl Phys Lett, 2008, 92: 092120

13 Wang D S, Zheng Y J. Quantum interference in a four-level system of a ^{87}Rb atom: Effects of spontaneously generated coherence. Phys Rev A, 2011, 83: 013810

14 Kang H S, Hernandez G, Zhang J P, et al. Phase-controlled light switching at low light levels. Phys Rev A, 2006, 73: 011802

15 Kang H, Kim J S, Hwang S I, et al. Electromagnetically induced trΛ-, and cascade-type schemes beyond steady-state analysis. Phys Rev A. 2005, 71: 053806

16 Hao X Y, Li J H, Ding C L, et al. Phase-dependent gain and absorption properties of mid- to infrared lights in three-coupled-quantum-wells. Opt Commun, 2009, 282: 4276–4282

17 Maichen W, Gaggl R, Korsunsky E, et al. Observation of phase-dependent coherent population trapping in optically closed atomic systems. Europhys Lett, 1995, 31: 189–194